Theoretical and Experimental Waveguide Characterization of Small Wire Scatterers

Jens Reinert, *Associate Member, IEEE,* and Arne F. Jacob, *Member, IEEE*

***Abstract*—A simple method is presented in this paper that allows us to verify numerically obtained polarizability tensors of electrically small scatterers by waveguide measurements. To this end, a model of the scattering process within the waveguide is developed. Measurements performed on a small helix in two different waveguide setups are compared to the theoretical data obtained from the model. A good agreement is demonstrated. Furthermore, the measured data are highly sensitive to the orientation of the scatterer within the waveguide. Thus, the polarizability tensors can be verified.**

***Index Terms*—Microwave measurements, perturbation methods, scattering parameter measurement, wire scatterers.**

I. Introduction

In the last two decades, artificial materials made of electrically small wire scatterers have been discussed intensively. Both numerical and experimental methods were developed in order to determine the material properties, i.e., the constitutive parameters [1]–[4]. In the experiments, a large amount of scatterers that form the material under investigation is measured [3], [5]. In contrast, most of the numerical methods use results obtained for only one scatterer (usually its polarizability tensors) and calculate the material properties by means of effective medium (or mixing) theories [1], [6]. Thus, the numerical tools can only be verified indirectly and it is nearly impossible to distinguish between errors introduced by the initial numerical calculations, the mixing theory, inhomogeneities within the material, and/or geometrical variations of the scatterers, whereas the latter two are always present in practical applications [5], [7].

In the following, a simple waveguide measurement method is used to determine the scattering parameters of a single electrically small wire scatterer (or obstacle) in dependence of its orientation in the waveguide. In order to be able to interpret these measurements, a model of the scattering process is developed. Provided the multipolarizability tensors of the obstacle are known (e.g., from the numerical calculations mentioned above), the scattering response can be calculated from this model. Hence, a direct and orientation-dependent verification of the numerically obtained polarizability tensors is possible. Since the scatterer in the waveguide is reduced to its polarizabilities, the equations obtained from the model are quite similar to those arising from Bethe's small aperture coupling theory [8].

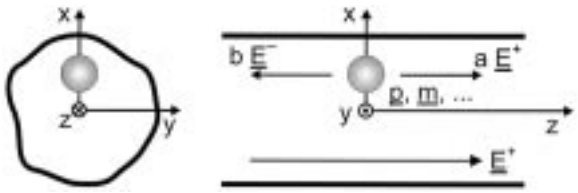

Fig. 1. Scatterer within the waveguide.

Previous investigations of single electrically small wire scatterers (or obstacles), as reported in [9], showed a very good agreement between the calculated and measured orientation-dependent radar cross sections of the wire structures. To this end, the scattered far field was calculated from the total current flowing on the wire and compared to free-space measurements. In contrast to these investigations, the method presented here focuses on the verification of the polarizability tensors of the obstacle; thus, the scattering response, i.e., the scattering parameters, of the obstacle must be accurately measured with respect to magnitude and phase. As will be shown, this goal can be reached by using a calibrated and electromagnetically well shielded waveguide setup.

II. Model

Consider a perfectly electrically conducting (PEC) cylindrical waveguide of arbitrary cross section S, whose longitudinal axis coincides with the z-axis of a Cartesian coordinate system (Fig. 1). The fundamental mode of such a waveguide is always a TE (or TEM) wave. The fields of this fundamental mode can be written as [8]

$$\underline{E}_0^{\pm} = \left\{ \begin{matrix} a \\ b \end{matrix} \right\} \underline{E}^{\pm} = \left\{ \begin{matrix} a \\ b \end{matrix} \right\} \underline{e} e^{\mp j k_z z}$$

$$\underline{H}_0^{\pm} = \left\{ \begin{matrix} a \\ b \end{matrix} \right\} \underline{H}^{\pm} = \left\{ \begin{matrix} a \\ b \end{matrix} \right\} (\underline{h}_z \pm \underline{h}) e^{\mp j k_z z}. \qquad (1)$$

Here, the superscript $+$ ($-$) refers to forward (backward) traveling waves (with respect to the positive z-direction), a (b) is the corresponding field amplitude, and k_z is the wavenumber along z. The transverse field components are given by $\underline{e}$ and $\underline{h}$, and $\underline{h}_z$ is the possible longitudinal component in the TE case. The model developed in the following is restricted to fundamental mode propagation and interaction; furthermore, power normalized fields are assumed, i.e.,

$$\int_S (\underline{e} \times \underline{h})_z \, dS = 1.$$

Manuscript received November 17, 2000.

The authors are with the Institut für Hochfrequenztechnik, Technische Universität Braunschweig, 38023 Braunschweig, Germany (e-mail: J.Reinert@tu-bs.de).

Publisher Item Identifier S 0018-9480(01)05056-6.

Using Schelkunoff's field equivalence principle [8] and image theory, any scatterer (including PEC wires, dielectric bodies, or coupling holes) within the waveguide can be modeled as a surface current density $\underline{J}$ radiating into the waveguide. According to [8], the magnitudes of the scattered waves excited by this current density $\underline{J}$ can be calculated as

$$2\begin{Bmatrix} a \\ b \end{Bmatrix} = -\int_V \underline{J}\cdot\underline{E}^{\mp}\,dV \tag{2}$$

where V is a volume containing $\underline{J}$. The integral on the right-hand side can be expanded into a multipole series to give

$$2\begin{Bmatrix} a \\ b \end{Bmatrix} = -j\omega\underline{E}^{\mp}\cdot\underline{p}+j\omega\underline{H}^{\mp}\cdot\underline{m}-\frac{j\omega}{2}\nabla\underline{E}^{\mp}\colon\underline{\underline{q}}+\ldots \tag{3}$$

with $\underline{p}$, $\underline{m}$, and $\underline{\underline{q}}$ as the electric and magnetic dipole moment, and the electric quadrupole moment of the scatterer, respectively. The double-dot product ":" is defined according to

$$\underline{\underline{A}}\colon\underline{\underline{B}} = \sum_{i=1}^{3}\sum_{j=1}^{3} A_{ij}B_{ji}.$$

The multipole moments are connected to the multipolarizability tensors by microscopic constitutive equations [10]. They read up to the electric quadrupole

$$\begin{aligned}
\underline{p} &= \underline{\underline{\alpha}}^{ee}\cdot\underline{E}+\underline{\underline{\alpha}}^{em}\cdot\underline{H}+\tfrac{1}{2}\underline{\underline{\underline{\tilde{Q}}}}^{ee}\colon\nabla\underline{E}\\
\underline{m} &= \underline{\underline{\alpha}}^{me}\cdot\underline{E}+\underline{\underline{\alpha}}^{mm}\cdot\underline{H}+\tfrac{1}{2}\underline{\underline{\underline{\tilde{Q}}}}^{me}\colon\nabla\underline{E}\\
\underline{\underline{q}} &= \underline{\underline{\underline{Q}}}^{ee}\cdot\underline{E}+\underline{\underline{\underline{Q}}}^{em}\cdot\underline{H}
\end{aligned} \tag{4}$$

where $\underline{E}$ and $\underline{H}$ are the fields that excite the scatterer. The symbols $\underline{\underline{\alpha}}^{\gamma\delta}$ and $\underline{\underline{\underline{Q}}}^{\gamma\delta}$ (or $\underline{\underline{\underline{\tilde{Q}}}}^{\gamma\delta}$) denote the different dipole and quadrupole polarizability tensors, respectively. The superscript δ indicates the electric ("e") or magnetic ("m") origin of the polarizability and $\gamma = 'e', 'm'$ stands for its electric or magnetic effect. If the scatterer is reciprocal—which is always the case for a PEC wire—the following symmetry relations hold for the different dipole and quadrupole polarizability tensors [10]:

$$\alpha_{ij}^{\gamma\delta} = \pm\alpha_{ji}^{\delta\gamma} \quad Q_{ijk}^{\gamma\delta} = Q_{jik}^{\gamma\delta} = \pm\tilde{Q}_{kij}^{\delta\gamma}. \tag{5}$$

The upper sign applies if $\gamma = \delta$, the lower if $\gamma \neq \delta$. Note that any further expansion of (4) has to be complete in the sense of the symmetry relations given in [10], otherwise reciprocity is not fulfilled and the results become inconsistent.

Now, let a forward-traveling fundamental mode of unit amplitude be incident on the scatterer. If the disturbance is small, $\underline{E}$ and $\underline{H}$ in (4) can be approximated by the undisturbed fundamental mode fields. With this assumption, the scattering parameters of the inclusion turn out to be

$$S_{11} = b = -\frac{j\omega}{2}\left(\underline{E}^{+}\cdot\underline{p}^{+}-\underline{H}^{+}\cdot\underline{m}^{+}+\frac{1}{2}\nabla\underline{E}^{+}\colon\underline{\underline{q}}^{+}\right) \tag{6}$$

$$S_{21} = 1+a = 1-\frac{j\omega}{2}\left(\underline{E}^{-}\cdot\underline{p}^{+}-\underline{H}^{-}\cdot\underline{m}^{+}+\frac{1}{2}\nabla\underline{E}^{-}\colon\underline{\underline{q}}^{+}\right). \tag{7}$$

Here, $\underline{p}^{+}$, $\underline{m}^{+}$, and $\underline{\underline{q}}^{+}$ are the multipole moments excited by the forward-traveling fundamental mode fields $\underline{E}^{+}$ and $\underline{H}^{+}$. This approximation gives results that are in good qualitative agreement with measurements. However, if the scatterer interacts more strongly with the fundamental mode, e.g., at resonance, the approach is likely to produce erroneous results. This is because the above approximation is not energy conservative. The latter can be proven by placing, for example, a lossless electrically small dielectric sphere ($\underline{\underline{\alpha}}^{ee} = \underline{\underline{I}}\alpha^{ee}$, $\mathrm{Im}\{\alpha^{ee}\} = 0$, all other tensors set to zero) in the waveguide; the energy condition for the lossless case $|S_{11}|^2 + |S_{21}|^2 = 1$ is not fulfilled.

This effect is also well known from the above-mentioned small aperture coupling theory [8]. To overcome this problem, the exciting fundamental mode fields in (4) have to be corrected. For a first-order approximation, these corrected fields can be found in the following way.

Consider the waveguide section $z < 0$ in Fig. 1. Far away from the scatterer, the fields consist of the incident and backscattered fundamental mode fields. If higher order modes are neglected, this statement remains valid even if one approaches $z = 0$. Thus, the fields that excite the inclusion must be

$$\underline{E} = \underline{E}^{+} + b\underline{E}^{-} \quad \underline{H} = \underline{H}^{+} + b\underline{H}^{-}. \tag{8}$$

The same arguments yield for $z > 0$

$$\underline{E} = \underline{E}^{+} + a\underline{E}^{+} \qquad \underline{H} = \underline{H}^{+} + a\underline{H}^{+}. \tag{9}$$

Within the correction procedure applied to the small aperture coupling theory, the average of these two fields is taken as the excitation. This is necessary to allow for waveguides of different cross section on either side of the coupling hole. The resulting expression for the wave amplitudes and scattering parameters then contains additional terms involving (very small) products of polarizabilities. Since the waveguide considered here is uniform, it is not necessary to perform this last step.

Applying the correction (8) when calculating b from (3) and (9) for the computation of a gives

$$b = \frac{-j\omega\underline{E}^{+}\cdot\underline{p}^{+} + j\omega\underline{H}^{+}\cdot\underline{m}^{+} - \frac{1}{2}j\omega\nabla\underline{E}^{+}\colon\underline{\underline{q}}^{+}}{2 + j\omega\underline{E}^{+}\cdot\underline{p}^{-} - j\omega\underline{H}^{+}\cdot\underline{m}^{-} + \frac{1}{2}j\omega\nabla\underline{E}^{+}\colon\underline{\underline{q}}^{-}} \tag{10}$$

$$a = \frac{-j\omega\underline{E}^{-}\cdot\underline{p}^{+} + j\omega\underline{H}^{-}\cdot\underline{m}^{+} - \frac{1}{2}j\omega\nabla\underline{E}^{-}\colon\underline{\underline{q}}^{+}}{2 + j\omega\underline{E}^{-}\cdot\underline{p}^{+} - j\omega\underline{H}^{-}\cdot\underline{m}^{+} + \frac{1}{2}j\omega\nabla\underline{E}^{-}\colon\underline{\underline{q}}^{+}} \tag{11}$$

where $\underline{p}^{-}$, $\underline{m}^{-}$, and $\underline{\underline{q}}^{-}$ are the multipole moments excited by the backward traveling fundamental mode fields $\underline{E}^{-}$ and $\underline{H}^{-}$. The scattering parameters are

$$S_{11} = \frac{-j\omega\underline{E}^{+}\cdot\underline{p}^{+} + j\omega\underline{H}^{+}\cdot\underline{m}^{+} - \frac{1}{2}j\omega\nabla\underline{E}^{+}\colon\underline{\underline{q}}^{+}}{2 + j\omega\underline{E}^{+}\cdot\underline{p}^{-} - j\omega\underline{H}^{+}\cdot\underline{m}^{-} + \frac{1}{2}j\omega\nabla\underline{E}^{+}\colon\underline{\underline{q}}^{-}} \tag{12}$$

$$S_{21} = \frac{2}{2 + j\omega\underline{E}^{-}\cdot\underline{p}^{+} - j\omega\underline{H}^{-}\cdot\underline{m}^{+} + \frac{1}{2}j\omega\nabla\underline{E}^{-}\colon\underline{\underline{q}}^{+}} \tag{13}$$

and they satisfy the energy conservation law.

These expressions differ from (6) and (7) by their denominators. These denominators are identical, though, because of the properties of the fundamental mode (1) and the symmetry relations (5). Therefore, it makes no difference whether corrections (8) or (9) are used alone or simultaneously, as was done here. This is a direct consequence of the continuity of the tangential fields at $z = 0$. Indeed, from (10) and (11), together with (1) it can be shown that an electric dipole within the waveguide leads to $a = b$. As can be seen from (8) and (9), this results in the correct boundary conditions for the fields in the plane of the scatterer (continuous tangential electric field, discontinuous tangential magnetic field). Similarly, a purely transverse magnetic dipole causes $a = -b$ (discontinuous tangential electric field, continuous tangential magnetic field). For very small interaction and if products of multipole moments are neglected, (12) and (13) become (6) and (7).

The remaining scattering parameters S_{22} and S_{12} can be obtained from (12) and (13), respectively, by changing the superscript $+$ $(-)$ to $-$ $(+)$. Of course, $S_{21} = S_{12}$, as required for a reciprocal scatterer.

III. Measurements and Comparison to Numerical Results

Measurements were performed in two different waveguide systems: A circular waveguide setup (30-mm waveguide diameter) and a circular coaxial setup (diameter of inner/outer conductor: 10/40 mm). The scatterer was a three-turn copper helix of 4-mm diameter and 4-mm height embedded in a polyurethan (PU)-foam sphere of 6-mm diameter [5]. In both waveguides, the helix was positioned by means of a 5-mm-thick Rohacell foam plug. For the circular waveguide measurements, the helix was located on the waveguide axis. In the coaxial setup, it was fixed halfway between the inner and outer conductors. The scattering parameters S_{11} and S_{21} were measured using a thru-reflect line (TRL)-calibrated [11] HP8510C network analyzer. Since the obstacles investigated in the following are small, S_{11} is also small, while S_{21} is close to unity. For both scattering parameters, the uncertainty of the measured phase increases with decreasing magnitudes. As a consequence, the phase of S_{21} is measured with a higher accuracy than that of S_{11}.

The theoretical polarizabilities of the helix were calculated using the method described in [6]. All polarizabilities appearing in (4) were taken into account for the calculations of the scattering parameters. The polarizability tensors obtained from [6] refer to a reference Cartesian coordinate system, thus, any reorientation can be realized by rotating this reference coordinate system into the desired direction. Since the helix with its surrounding sphere is not a point scatterer, as required by the theory, the modal fields at the center of the sphere were taken as the exciting fields. In all experiments, the electric-field vector of the exciting fundamental mode pointed in the x-direction (see Fig. 1).

Figs. 2 and 3 show the measured and calculated scattering parameters S_{11} and S_{21} for a helix with its axis parallel to the x-axis. The wire ends are in the xy-plane. The frequency band displayed contains the $\lambda/2$-resonance of the helix. For S_{11}, theoretical and measured values agree very well as long as the magnitude is larger than -30 dB. In order to demonstrate the effect of the correction introduced in the previous section, the magnitude of S_{11} was calculated with and without it. Since energy conservation is violated in the latter case, the measured magnitude is overestimated, especially at resonance. In order to avoid these effects, the correction is applied to all following calculations. The theoretical values of S_{21} (Fig. 3) reproduce the measured ones within the typical measurement accuracy (magnitude: ± 0.1 dB, phase: $\pm 2^{\circ}$).

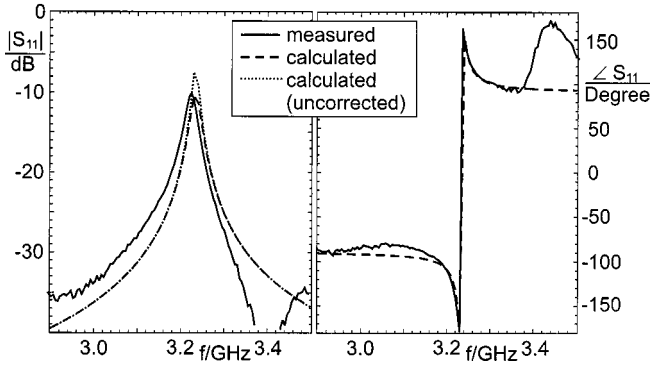

Fig. 2. Scattering parameter S_{11} (helix axis parallel to x-axis).

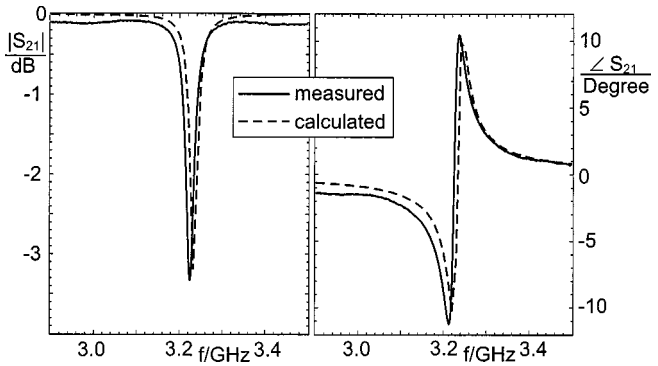

Fig. 3. Scattering parameter S_{21} (helix axis parallel to x-axis).

The small resonance shift visible in Figs. 2 and 3 is mainly caused by the following two effects. First, numerical errors introduced when calculating the polarizabilities shift the resonance (for a discussion, see [6]). Second, the helix dimensions are known within a tolerance margin, only. These tolerances are caused by the manufacturing process and can lead to the above shift [7].

Fig. 4 displays S_{21} measured and calculated for two helices with their axes pointing in the y- and z-directions, respectively. The achieved measurement (or calculation) accuracy is the same as in Fig. 3. A comparison of the S_{21} values obtained for the three different helix orientations depicted in Figs. 3 and 4 (and the corresponding values of S_{11} that are not shown here) indicate that an orientation-dependent verification of the polarizability tensors is possible.

To further demonstrate this ability, Fig. 5 displays S_{11} measured and calculated in a frequency band centered at the λ-resonance of the helix. The helix axis was parallel to the z-axis. The calculations show that the measurement value is mainly caused by the quadrupole polarizabilities of the helix. Neglecting

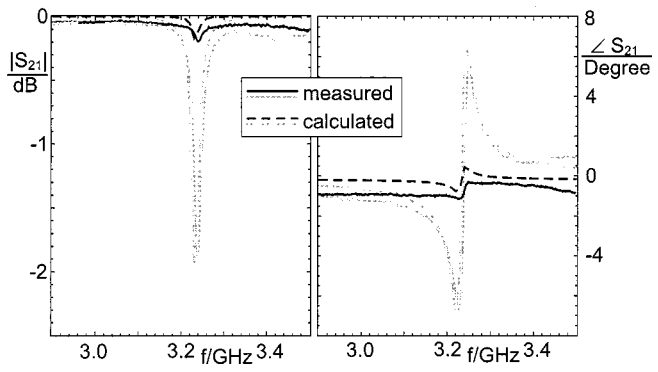

Fig. 4. Scattering parameter S_{21} for two different helix orientations: Grey lines: helix axis pointing in y-direction. Black lines: helix axis parallel to waveguide axis.

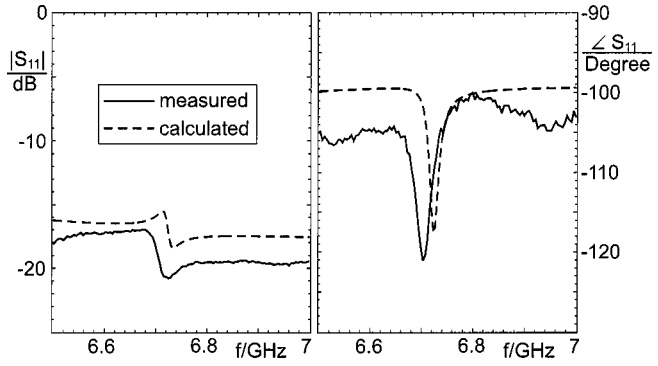

Fig. 5. Scattering parameter S_{11} at the λ resonance (helix axis parallel to waveguide axis).

the quadrupole polarizabilities in the calculations would lead to the completely wrong result $S_{11} \approx 0 (S_{11} \approx -45$ dB). Thus, the model enables one to distinguish not only between different scattering responses due to the helix orientation, but also due to different polarizability terms. It should be noted that the scattering parameters of Figs. 2–4 are also affected by the quadrupole polarizabilities. However, their effect is not as pronounced as in Fig. 5 and can be neglected in most cases.

IV. Discussion and Conclusion

The simple model of the scattering process described in this paper is very easy to implement and produces results in very good agreement with waveguide measurements. It has been demonstrated that measured and calculated scattering responses are highly sensitive to the orientation of the obstacle within the waveguide. Furthermore, effects caused by different polarizability tensors and multipole moments are distinguishable. Thus, the combination of the model and the waveguide measurements yields a simple and accurate tool that allows verification of numerically obtained polarizabilities.

Theoretically, the model enables one to determine the components of the polarizability tensors from measurements. Indeed, it is easy to invert the formulas for the scattering parameters in order to calculate the different tensor components from measured data. A full characterization would require the repeated reorientation of the scatterer within the waveguide. Scattering parameters obtained from different orientations must then be combined to isolate the effects caused by a single tensor component. However, for the implementation of this procedure, a redesign of the measurement setup is needed so that the scatterer can be positioned with higher accuracy and reproducibility.

References

[1] C. R. Brewit-Taylor, P. G. Lederer, F. C. Smith, and S. Haq, "Measurement and prediction of helix-loaded chiral composites," *IEEE Trans. Antennas Propagat.*, vol. 47, pp. 692–700, Apr. 1999.

[2] K. W. Whites, "Full-wave computation of constitutive parameters for lossless composite chiral materials," *IEEE Trans. Antennas Propagat.*, vol. 43, pp. 376–384, Apr. 1995.

[3] I. P. Theron and J. H. Cloete, "The electric quadrupole contribution to the circular birefringence of nonmagnetic anisotropic chiral media: A circular waveguide experiment," *IEEE Trans. Microwave Theory Tech.*, vol. 44, pp. 1451–1459, Aug. 1996.

[4] J. Reinert, G. Busse, and A. F. Jacob, "Waveguide characterization of chiral material: Theory," *IEEE Trans. Microwave Theory Tech.*, vol. 47, pp. 290–296, Mar. 1999.

[5] G. Busse, J. Reinert, and A. F. Jacob, "Waveguide characterization of chiral material: experiments," *IEEE Trans. Microwave Theory Tech.*, vol. 47, pp. 297–301, Mar. 1999.

[6] J. Reinert and A. F. Jacob, "Direct calculation of the multi-polarizability tensors for thin-wire scatterers," *IEEE Trans. Antennas Propagat.*, to be published.

[7] J. Psilopoulos, J. Reinert, and A. F. Jacob, "Fabrication effects on the resonance bandwidth of chiral materials," in *Proc. Bianisotrop.*, Lisbon, Portugal, Sept. 2000, pp. 313–316.

[8] R. E. Collin, *Field Theory of Guided Waves*, 2nd ed. Piscataway, NJ: IEEE Press, 1991.

[9] F. Mariotte, S. A. Tretyakov, and B. Sauviac, "Modeling effective properties of chiral composites," *IEEE Antennas Propagat. Mag.*, vol. 38, pp. 22–32, Feb. 1996.

[10] E. B. Graham and R. E. Raab, "Light propagation in cubic and other anistropic crystals," *Proc. R. Soc. Lond. A, Math. Phys. Sci.*, vol. 430, pp. 593–614, 1990.

[11] "Applying the HP 8510B TRL calibration for noncoaxial measurements," Hewlett-Packard Company, Santa Rosa, CA, Product Note 8510-8, 1987.

Jens Reinert (S'95–A'96) was born in Einbeck, Germany, in 1970. He received the Dipl.-Ing. degree from the Technische Universität Braunschweig, Braunschweig, Germany, in 1995, and is currently working toward the Ph.D. degree at the Technische Universität Braunschweig.

Since 1997, he has been a Member of the Research Staff at the Institut für Hochfrequenztechnik, Technische Universität Braunschweig. His research interests include electromagnetic theory, wave propagation in complex materials, and numerical methods in electromagnetics.

Arne F. Jacob (S'79–M'81) was born in Braunschweig, Germany, in 1954. He received the Dipl.-Ing. and Dr.-Ing. degrees from the Technische Universität Braunschweig, Braunschweig, Germany, in 1979 and 1986, respectively.

From February 1986 to January 1988, he was a Fellow at the European Laboratory for Particle Physics (CERN), Geneva, Switzerland. From February 1988 to September 1990, he was with the Accelerator and Fusion Research Division, Lawrence Berkeley Laboratory, University of California at Berkeley. Since 1990, he has been a Professor at the Institut für Hochfrequenztechnik, Technische Universität Braunschweig. His current research interests include the design and application of planar circuits at microwave and millimeter-wave frequencies, and the characterization of complex materials.